Exp Brain Res (2010) 200:51–60
DOI 10.1007/s00221-009-1990-3

RESEARCH ARTICLE

Visual selectivity for heading in monkey area MST

Frank Bremmer · Michael Kubischik · Martin Pekel · Klaus-Peter Hoffmann · Markus Lappe

Received: 3 June 2009 / Accepted: 8 August 2009 / Published online: 29 August 2009

Abstract The control of self-motion is supported by visual, vestibular, and proprioceptive signals. Recent research has shown how these signals interact in the monkey medio-superior temporal area (area MST) to enhance and disambiguate the perception of heading during self-motion. Area MST is a central stage for self-motion processing from optic flow, and integrates flow field information with vestibular self-motion and extraretinal eye movement information. Such multimodal cue integration is clearly important to solidify perception. However to understand the information processing capabilities of the brain, one must also ask how much information can be deduced from a single cue alone. This is particularly pertinent for optic flow, where controversies over its usefulness for self-motion control have existed ever since Gibson proposed his direct approach to ecological perception. In our study, we therefore, tested macaque MST neurons for their heading selectivity in highly complex flow fields based on the purely visual mechanisms. We recorded responses of MST neurons to simple radial flow fields and to distorted flow fields that simulated a self-motion plus an eye movement. About half of the cells compensated for such distortion and kept the same heading selectivity in both cases. Our results strongly support the notion of an involvement of area MST in the computation of heading.

Keywords Macaque · Extrastriate · Optic flow · Parietal cortex

F. Bremmer · M. Kubischik · M. Pekel · K.-P. Hoffmann · M. Lappe
Allg. Zoologie und Neurobiologie,
Ruhr Universität Bochum, 44780 Bochum, Germany

F. Bremmer (✉)
AG Neurophysik, Philipps-Universität Marburg,
Renthof 7, 35032 Marburg, Germany
e-mail: frank.bremmer@physik.uni-marburg.de

M. Lappe
Psychologisches Institut II, Westfälische Wilhelms-Universität
Münster, Fliednerstr. 21, 48149 Münster, Germany

Introduction

Gibson (1950) proposed that the visual flow in the optic field surrounding a moving observer contained sufficient information to estimate heading just from invariances in the flow pattern itself. His further suggestion, however, that the focus of expansion in the flow is such an invariant is problematic, since the optic flow as sensed by the eyes is superimposed with tracking eye movements which distort the flow structure and destroy the focus of expansion (Fig. 1); such eye movements are reflexively induced by the flow itself, and attempt to stabilize the parafoveal image (Lappe et al. 1998; Wei and Angelaki 2006). Yet, human observers are able to estimate heading from such complex spiraling flow fields in the absence of a focus of expansion (Warren and Hannon 1988; Van den Berg 1993).

Cortical area MST of the macaque monkey has been implied in self-motion processing based on its selectivity to optic flow (Tanaka and Saito 1989; Duffy and Wurtz 1991a; Lagae et al. 1994) and vestibular self-motion cues (Bremmer et al. 1999; Froehler and Duffy 2002; Gu et al. 2006, 2008), and because microstimulation in MST influences the monkey's perceived direction of self-motion from optic flow (Britten and van Wezel 1998, 2002). The visual selectivity of MST neurons for the center of expansion in a radial flow field enables a population code in area MST to signal heading in the absence of eye movements (Lappe et al. 1996). This ability is partially preserved during

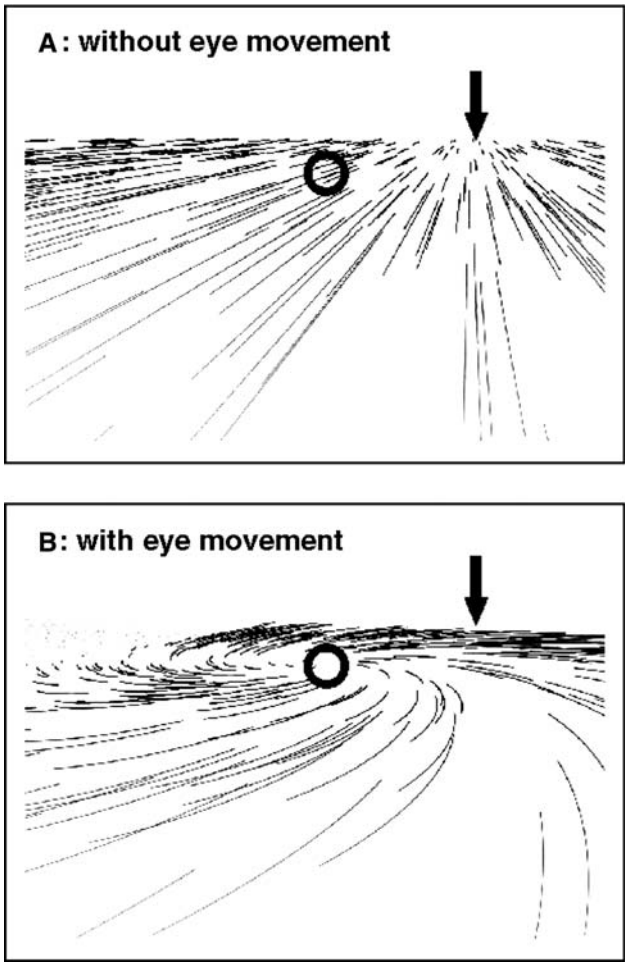

Fig. 1 Retinal flow fields seen by an observer moving in a rightward heading direction (*arrow*) on top of a ground plane. Both **a** and **b** display the same heading (*arrow*), but differ in terms of eye movements. **a** A radial expansion centered at the heading point. This pattern occurs in the absence of eye movements (gain = 0.0). **b** Eye movements that spontaneously occur in primates are included (gain = 1.0). These eye movements track the motion in the direction of gaze (*circle*) and distort the structure of the flow on the retina, generating a motion pattern that resembles a spiral and in which the motion in gaze direction (*circle*) is minimized. Invariant responses to heading should be the same in both cases, since heading is identical although flow structure is different

pursuit eye movements suggesting that MST neurons receive an extraretinal efference copy signal (Bradley et al. 1996; Page and Duffy 1999; Shenoy et al. 1999; Upadhyay et al. 2000). However, MST neurons also respond strongly to spiraling motion patterns (Graziano et al. 1994). This sensitivity might be related to a visual mechanism for heading estimation during eye movements that analyzes the distorted structure of the retinal flow induced by tracking eye movements and functions as a backup for the extraretinal process (Lappe and Rauschecker 1993; Perrone and Stone 1994). To test this hypothesis, we compared the selectivity of individual MST neurons to radial (Fig. 1a) and distorted (Fig. 1b) flow patterns that represent the same heading. Critically, we presented optic flow fields that simulated self-motion with respect to a flat horizontal plane because in this situation, the characteristic spiraling motion pattern occurs when tracking eye movements are added (Warren and Hannon 1988; Lappe and Rauschecker 1994). Stimuli simulated realistic, natural flow fields that are experienced during combined self-translation and eye rotation, or during self-translation alone, over a virtual horizontal plane.

Methods

We recorded from single cells in two hemispheres of two awake, behaving monkeys performing a fixation or free-viewing task. All procedures were conducted in accordance with the published guidelines on the use of animals in research (European Communities Council Directive 86/609/ECC).

Animal preparation

Experimental methods followed standard procedures that are described in more detail in (Bremmer et al. 1997; Lappe et al. 1998). In brief, the monkeys were surgically prepared for chronic neurophysiological recordings in the medio-superior temporal area (area MST). Under general anesthesia and sterile surgical conditions, each animal was implanted with a device for holding the head, scleral search coils for eye position monitoring (Judge et al. 1980) and a recording chamber for introducing electrodes into the brain. For recordings, in each animal, a stainless steel cylinder was placed over the occipital cortex in a parasagittal stereotaxic plane tilted 60° back from the vertical. In both monkeys, the exact location of the craniotomy was determined based on the pre-surgical MR scanning. Recording chamber, eye coil plugs and head holders were embedded in dental acrylic cap that itself was connected to the skull by self-tapping screws. Analgesics were applied postoperatively and recording started no sooner than a week after surgery.

Behavioral paradigm and recordings

Prior to the experiments, monkeys had been trained to fixate a red spot of light. During training and recording sessions, the monkeys' head was restrained on a primate chair while he was either performing a fixation task or was allowed to freely move his eyes. In trials that required fixation, the fixation target was always presented in the center of the screen and the monkey had to maintain central fixation within an electronically controlled window (2° diameter) throughout the stimulation period of 3.5 s. Horizontal and vertical eye positions were monitored with a search coil (see above) and sampled at 500 Hz. Single unit activity was

recorded using tungsten-in-glass electrodes and a hydraulic microdrive (Narishige Ltd., London, UK). In some experiments, a multielectrode recording system (Thomas Recording GmbH, Gießen, Germany) was used. In both cases, an online spike sorting system (MSD, Alpha Omega GmbH, Ubstadt-Weiher, Germany) was used to isolate multiple single unit data from a single electrode. Behavioral paradigm, visual stimulation, and data acquisition were controlled by a PC. At the end of the training or experimental sessions, the monkey was returned to his home cage. Monkey's weight was monitored daily and supplementary fruit or water supply was provided whenever necessary.

Visual stimuli

Optic flow stimuli were generated in OpenGL with a frame rate of 72 Hz. The stimuli consisted of full field computer-generated sequences that were back projected via a video projector onto a tangent screen, 48 cm in front of the monkey. The size of the projection covered the central $\pm 45° \times \pm 45°$ of the visual field. Optic flow sequences simulated ego motion of a virtual observer over an extended horizontal plane located 37 cm below eye level. The plane was either covered with a texture pattern or with a random arrangement of white dots on a dark background. Trials simulated self-motion at 1 m/s in one of three directions (30° to the left, straight-ahead, 30° to the right) and sometimes included simulated eye movements as explained below. Simulated eye movements were similar to naturally occurring tracking movements (Lappe et al. 1998). Simulated eye speed increased during the trial according to the increase in speed of the tracked object in the flow as it got nearer. In the trials with the fastest simulated eye movement, eye speed had a median of 3.7° per s and reached 11° per s towards the end of the trial. During recordings, the three different self-motion directions were combined with three different gains 'g' of the simulated eye movement [$g = 0.0$ (fixed gaze), $g = 0.5$ (aiming at the natural viewing behavior) (Lappe et al. 1998), and $g = 1.0$ (imitating perfect tracking of a target on the ground plane)]. These three-by-three = nine different stimulus conditions were presented in pseudo-randomized order across trials and were combined with blocks of trials where the animal was allowed to perform spontaneous, unrestrained eye movements. As for the simulated eye movement conditions also, three different self-motion directions (30° to the left, straight-ahead, 30° to the right) were presented in pseudo-randomized order across trials.

The determination of receptive field location and general response properties of a neuron used the following procedure. We first determined the directional tuning for full field unidirectional motion by moving a large Julesz pattern on a circular pathway within the frontal plane (Schoppmann and Hoffmann 1976; Bremmer et al. 1997, 2002). This method allows in determining a neuron's directional selectivity in a single run, using the phase of the motion as a determinant of direction. A movie which is similar to the stimulus used in our experiments can be seen at http://www.physik.uni-marburg.de/en/research/neurophysik/group-bremmer/circular-pathway-stimuli.html (Actually, there are three movies on this website: one showing movement in the frontal plane (as used in the current study), and two others showing movements in the horizontal and in the sagittal plane.) We then determined the RF for local image motion in a direction close to the preferred direction with small field stimuli as described in (Duhamel et al. 1997) and (Schlack et al. 2005). To this end, a single moving luminant bar was presented in one of 36 $10° \times 10°$ patches of the central $60° \times 60°$ of the screen for 200 ms followed by 200 ms of a dark screen. Then, the bar was presented at another pseudo-randomly chosen location for 200 ms, followed by a dark period of 200 ms, etc. Six stimulus movements, each followed by a dark period, were presented during the course of a single trial. Typically, neural responses for 5–10 stimulus repetitions at each patch location were recorded.

Data analysis

Trials with simulated eye movements (duration = 3,500 ms) were sorted offline according to their self-motion direction and their simulated gain. A distribution-free analysis of variance was computed to determine significant responses and tunings of the cells. Trials in the free-eye movement condition had a duration of 20 s. Eye movements were analyzed using earlier developed methods (Lappe et al. 1998). Fast eye movements were detected by an eye velocity criterion (threshold set to $v_{th} = 60°$ per s). Neural activity in the tracking phases between two such fast eye movements was analyzed in the following way. First, all tracking phases in which eye position was outside the central $\pm 10°$ by $\pm 10°$ of the screen were discarded to avoid possible contamination of neural activity by eye position signals or screen border effects. Afterwards, all remaining tracking phases were temporally aligned to the onset of the preceding fast eye movement. Then, average neural activity in 20 ms bins was determined across all tracking phases. Because we used only tracking phases in which the eye position was within the central 10° of the stimulus the resulting eye movements within each stimulus were very similar to each other and could be easily averaged.

For a population analysis, neural activity for all simulated eye movement gains was ranked according to each neuron's response for a given self-motion direction. As an example, if a neuron showed its largest response for leftward motion, irrespective of the simulated eye movement,

the rank order for leftward movement was 1-1-1. If, at the same time, the second largest response was obtained for straight-ahead motion, this resulted in a rank 2-2-2. This, in turn, implied that the weakest responses were obtained for simulated rightward motion, resulting in a rank 3-3-3. In summary, the response of each neuron resulted in three rank profiles, one for each self-motion direction. The total number of ranks was, therefore, three times the number of neurons tested in this task. This analysis did not consider, however, the eye movement condition (gain) for which a given rank was obtained. In other words, rank orders 1-1-2, 1-2-1, and 2-1-1 were considered to be identical. This analysis, therefore, led to a total of 10 possible rank orders (1-1-1, 2-2-2, 3-3-3, 1-1-2, 1-1-3, 1-2-2, 1-3-3, 2-2-3, 2-3-3, 1-2-3). If responses across eye movement conditions had been unrelated, we had expected a uniform distribution of rank orders (10% each). If neurons, however, would prefer specific self-motion directions irrespective of the simulated eye movement, we would expect a higher proportion of responses with rank orders 1-1-1, 2-2-2, and/or 3-3-3.

Location and extent of the receptive field were calculated by temporally correlating the firing rate with the location of the bar, corrected for the latency of the neuron.

Results

We recorded single unit activity of 84 MST cells from two awake-behaving monkeys during exposure to optic flow fields. During recordings, neurons were not preselected, i.e. we recorded from any neuron that could be activated by visual stimulation. Area MST was identified based on the recording depth and neural response properties (middle sized to large visual RF, strong directional selectivity for visual motion). Histological analysis in one animal verified that recording sites had been located throughout area MST, including the dorsal and the ventral aspects, i.e. areas MSTd and MSTl, respectively. We determined the sensitivity of individual neurons to different optic flow patterns resulting from combinations of eye movement and heading. Stimuli simulated realistic, natural flow fields that are experienced during combined self-translation and eye rotation, or during self-translation alone, over a virtual horizontal plane of 37 cm below the eye level. Three different headings, straight-ahead or 30° left or right, were tested in each of four eye movement conditions, i.e. during fixation (gain of the eye movement is $g = 0.0$), with two simulated eye movements ($g = 0.5$, $g = 1.0$), and with real eye movements; 61/84 (72%) of the neurons showed a statistically significant response in at least one of the simulated eye movement conditions ($g = 0.0$, 0.5, and 1.0); 54/84 (64%) neurons responded statistically significant for real and simulated eye movement conditions. Many of these neurons favored a single heading in all four (no, simulated, and real) eye movement conditions. A representative example is shown in Fig. 2 (see also Table 1). This neuron consistently preferred rightward heading. It responded invariantly to the direction of self-motion (rightward) and was unaffected by simulated eye movements (Fig. 2a–c). This invariance must be achieved by visual motion processing properties of the neuron because it is seen even when the eyes are physically stationary, i.e. when eye movements are only simulated and an efference copy signal is not available. The modulation of firing rate was significantly lower in the real eye movement condition than in any of the simulated eye movement conditions (Fig. 2d, e). This finding was quite common in area MST as can be seen in Fig. 3. In this scatter plot, each data point indicates the difference in neural activity (response modulation) between the strongest and the weakest response of an individual neuron for simulated (abscissa) and real (ordinate) eye movements. Response modulation was larger for simulated when compared with real eye movements in 37/54 neurons (69%), making this difference statistically significant ($P < 0.005$, Mann–Whitney rank sum test).

About half of the neurons (40/84) we tested responded best to the same heading in all conditions. Of the remaining neurons, some responded best to a certain heading in one condition, but lost their selectivity to heading in others. One such example is shown in Fig. 4. This neuron had no heading preference, neither in the no eye movement condition (gain = 0.0, row A) nor in the eye movement condition with small gain (gain = 0.5, row B). In the full gain condition (gain = 1.0, row C), however, this neuron showed a clear and reproducible preference for forward motion (straight-ahead, middle panel). The ramp-like activity increase during the course of the trial can be explained by the retinal stimulation, which turns into a full field radial expansion during the approach towards the virtual target on the ground plane which is tracked by the simulated eye movements.

We aimed to quantify this stability (like in Fig. 2) or variability (like in Fig. 4) of the neurons' tuning across eye movements. To this end, we ranked the response strength of each individual neuron for each simulated eye movement condition (gain $g = 0.0$, 0.5, and 1.0). As an example for response invariance as shown in Fig. 2, discharges in the 'no eye movement condition' ($g = 0.0$; top row) were $resp_{right} = 40.5$ Sp/s for rightward movement (rank = 1), $resp_{straight\text{-}ahead} = 4.6$ Sp/s for straight-ahead movement (rank = 2) and $resp_{left} = 4.2$ Sp/s for leftward movement (rank = 3). For a simulated gain of 50% ($g = 0.5$, middle row) as observed during spontaneous eye movements (Lappe et al. 1998) resulted in the following responses: $resp_{right} = 35.2$ Sp/s (rank = 1), $resp_{straight\text{-}ahead} = 6.3$ Sp/s for straight-ahead (rank = 2) and $resp_{left} = 6.2$ Sp/s for leftward

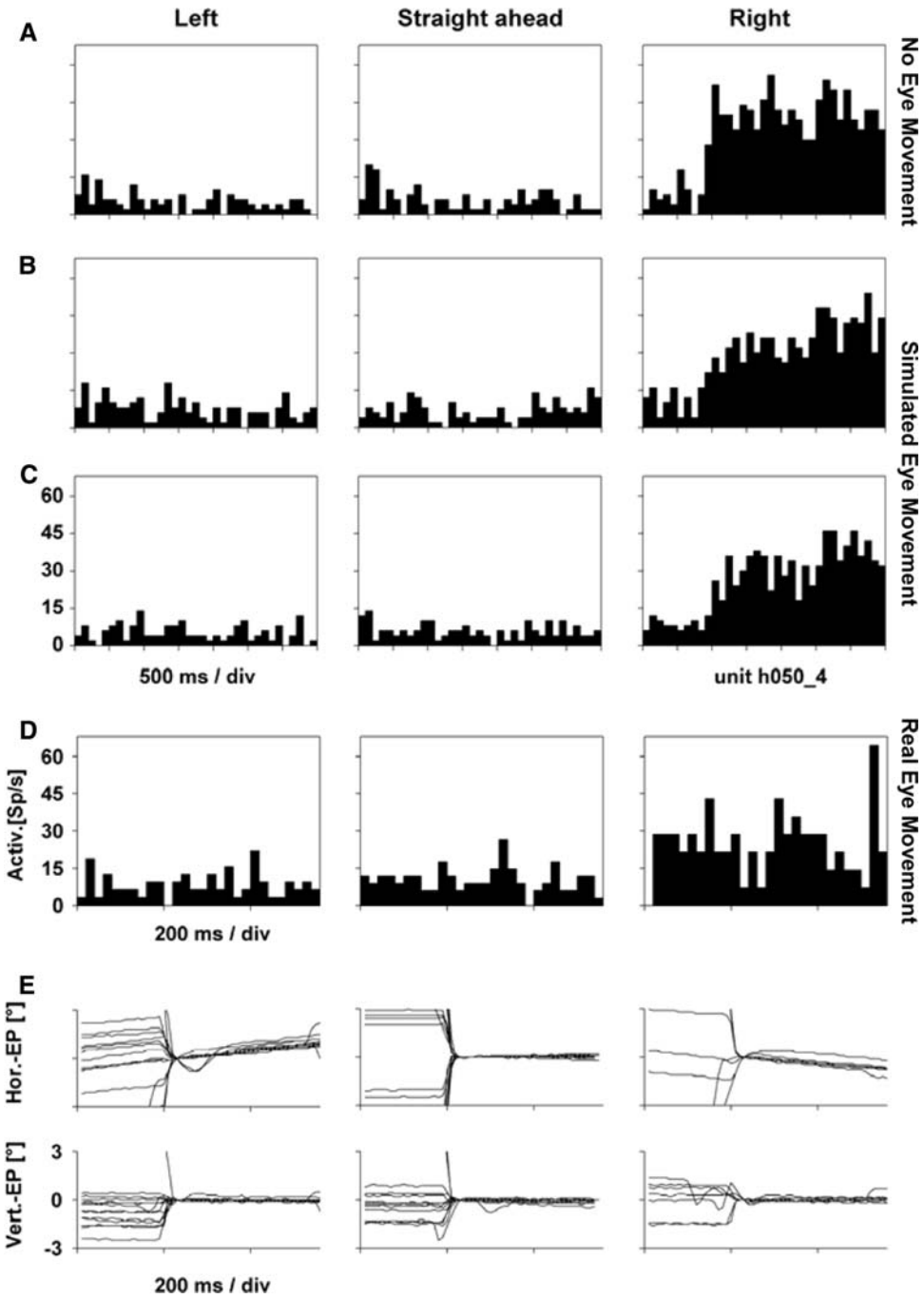

Fig. 2 A neuron responding to rightward heading irrespective of eye movements. *Histograms* show the neuron's firing rate over time during the presentation of optic flow stimuli. Columns from left to right present responses to leftward, forward, and rightward heading stimuli, respectively, for different eye movement conditions. **a**–**c** The animal continuously fixated a central target. **a** Optic flow stimuli consisted of simple radial motion simulating only observer translation with no additional simulated eye movements (gain = 0.0; see also Fig. 1a), **b**, **c** simulated the same observer motion, but included additional simulated eye movements that distorted the flow field (see also Fig. 1b). The eye movements simulated ocular tracking of visual motion in the flow field (indicated by the *circle* in Fig. 1) with a gain of 0.5 (**b**) or 1.0 (**c**). **d** Responses of the same cell during real eye movements while presenting radial flow on the screen. The animal in this case was looking near the area of the *circle* in Fig. 1a, but was performing spontaneous tracking eye movements. Because these eye movements add image motion on the retina, the actual retinal motion pattern is like the one in Fig. 1b. **e** Sample horizontal and vertical eye movement traces of the animal as observed in the free-eye movement condition. Neural activity and eye movement traces are aligned to the onset of the fast phase of the optokinetic like eye movement pattern. Note that the time scales are different in **a**–**c** and **d**–**e**. This re-scaling was necessary because reflexive fast phases during OKN occur every 300–500 ms (Lappe et al. 1998). These fast phases can modulate the ongoing neural activity (see e.g. extreme right in **d**)

Table 1 Mean discharges and response ranks

	Leftward	Straight-ahead	Rightward
Gain 0.0	4.2/3	4.6/2	40.5/1
Gain 0.5	6.2/3	6.3/2	35.2/1
Gain 1.0	5.0/3	5.6/2	32.2/1
	3-3-3	2-2-2	1-1-1

Data are taken from histograms shown in Fig. 2 (response window: 1,000–3,000 ms)

Each entry in the table gives the response in (spikes/s) and the resulting rank for a given eye movement gain

As an example: for gain 0.0, the discharge for rightward movement (40.5 Sp/s) was largest, leading to a rank value 1

For the same gain, the discharge 4.6 Sp/s (straight-ahead movement) resulted in rank 2, while the discharge 4.2 Sp/s (leftward movement) resulted in rank 3

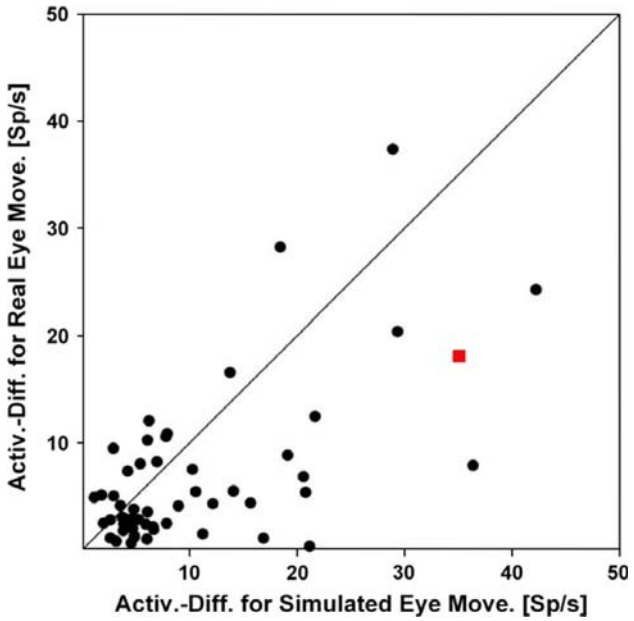

Fig. 3 Response modulation during real and simulated eye movements. During simulated (abscissa) and real (ordinate) eye movements each neuron had a strongest and a weakest response. For each neuron, we computed the difference of these two values defining a response modulation (RM). At the population level, RM was significantly stronger for simulated when compared with real eye movements ($n = 54$, $P < 0.005$, Mann–Whitney rank sum test). The *red square* indicates the RM value obtained from data in Fig. 2

movement (rank = 3). Finally, a simulated eye movement with optimal gain ($g = 1.0$, bottom row; imitating perfect tracking of a target on the ground plane), responses were $\text{resp}_{\text{right}} = 32.2$ Sp/s (rank = 1), $\text{resp}_{\text{straight-ahead}} = 5.6$ Sp/s (rank = 2) and $\text{resp}_{\text{left}} = 5.0$ Sp/s for leftward movement (rank = 3). Hence, the rank values obtained from the responses of this neuron were 1-1-1, 2-2-2, and 3-3-3 (see also Table 1). This invariance concerning simulated eye movements was typical for the population of neurons and was obtained in almost 45% of the responses (Fig. 5; 1-1-1: 17%; 2-2-2: 12%; 3-3-3: 17%). Of the remaining neurons some responded best to a certain heading in one condition, but lost their selectivity to heading in others (like in the example shown in Fig. 4; see also Table 2). Other neurons preferred different headings in the different simulated eye movement conditions. Neurons with a switch of their tuning from leftward to rightward (1-1-3: 4.9%, 1-3-3: 4.4%, 1-2-3: 3.3%, summing to a total of 12.6%) and vice versa were least frequently observed.

All cells that preferred the same heading both for simple radial flow and during real eye movements, also did so during simulated eye movements. Hence, the pattern of retinal motion appears the most important factor for the neuron's invariant response. The motion patterns with and without eye movements are particularly different in the area around the line of sight and along the horizon (see Fig. 1). Neurons that have their receptive fields in this area and that respond similarly to both flow fields must have complex response selectivities. In some of the neurons that showed consistent heading responses, we measured the location of the visual receptive field (RF) with small field unidirectional local image motion and compared it with those of the response behavior to optic flow. We found that the flow responses of some cells tolerated large changes in local image motion in their RF. Figure 6 shows an example in which heading selectivity is constant, despite a reversal of local image motion direction in the most sensitive part of the RF. This neuron does not only use local unidirectional image motion from the RF center, but a more complex selectivity for flow patterns, including summation from the peripheral parts of the RF and perhaps local speed selectivities. RF mechanisms that could generate such invariant heading responses have been proposed in several neural models for heading detection (Lappe and Rauschecker 1993; Perrone and Stone 1994; Beintema and Van den Berg 1998; Beintema et al. 2004).

Discussion

In summary, we have used the simulated eye movement techniques (Warren and Hannon 1988, 1990) to show that MST neurons respond selectively to heading irrespective of the occurrence of tracking eye movements, and, crucially, that this invariant response is derived from purely visual mechanisms. Our findings show that MST neurons can use visual information from the distorted retinal flow during combined self-motion and tracking eye movements to estimate heading. The ability to cope with the distorted flow fields is important because eye movements are common during natural self-motion (Lappe et al. 1998). In principle, there are two possibilities by which the visual system could

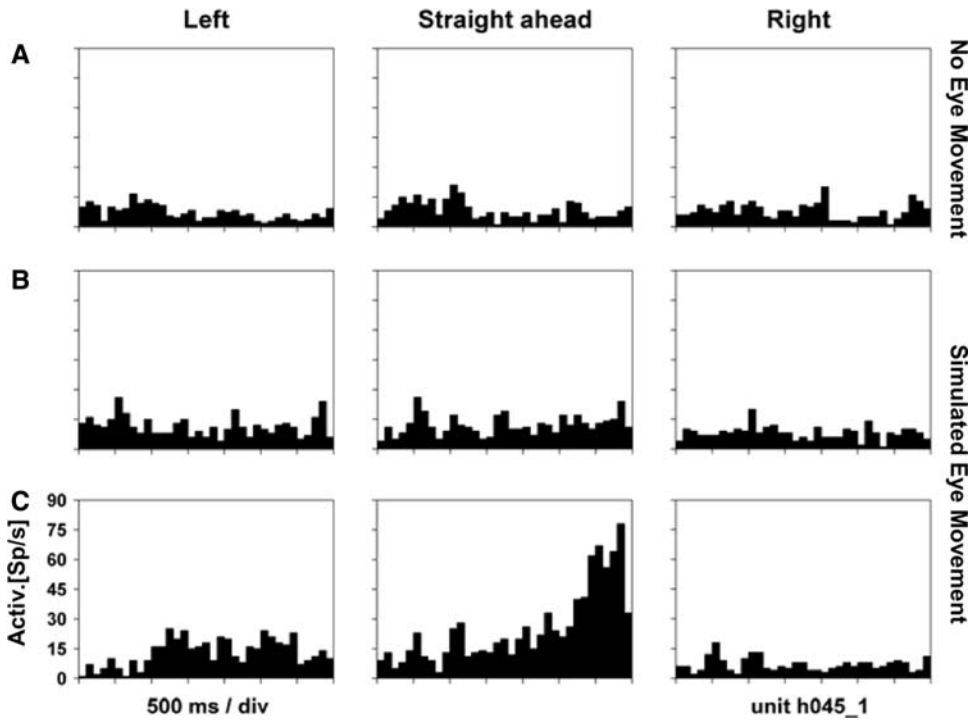

Fig. 4 A neuron responding to forward heading only during high-gain simulated eye movements. This neuron was not responsive for leftward or rightward heading. Instead, neural activity increased only during forward motion with additional simulated eye movements with gain 1.0. The ramp-like activity increase during the course of the trial can be explained by the retinal stimulation, which turns into a full field radial expansion during the approach towards the virtual target on the ground plane which is tracked by the simulated eye movements. This neuron was not tested during real eye movements

extract heading when retinal flow is distorted by eye movements. It could either use non-visual (extraretinal) information about the eye movement, or it could use the distorted structure of the retinal motion pattern itself. The use of extraretinal eye movement signals to compensate for the distortions that smooth pursuit eye movements introduce in retinal flow has often been shown (Bradley et al. 1996; Page and Duffy 1999; Shenoy et al. 1999; Upadhyay et al. 2000; Britten and van Wezel 2002), consistent with evidence of the use of such a signal in humans (Warren and Hannon 1990; Royden et al. 1992; Lappe et al. 1999). Humans, however, can also use the structure of the flow pattern directly. This is particularly true for travel over a horizontal ground plane and eye movements that simulate natural gaze stabilization mechanisms (Warren and Hannon 1988; Van den Berg 1993). In this case, the retinal flow pattern has a characteristic spiraling structure. Our results demonstrate that MST neurons can analyze this structure for retaining their heading selectivity during eye movements. Thus, area MST not only combines multimodal cues for heading in an optimal fashion (Page and Duffy 1999; Froehler and Duffy 2002; Gu et al. 2006, 2008; Morgan et al. 2008), but also exploits the information in the visual cue alone in a complex and elaborate manner.

Bradley et al. (1996), who tested MST neurons with both real and simulated eye movements, found that the neurons retained their heading selectivity only during real and not during simulated pursuit. This response behavior is somewhat similar to the 'real motion cells' as described for area MST (Erickson and Thier 1991) but also area V1 and other extrastriate areas (Galletti et al. 1984, 1988, 1990). However, the stimulus used in the study by Bradley et al. differed from our stimulus in that it simulated self-movement towards a frontoparallel plane, whereas we simulated movement on top of a ground plane. The stimulus used by Bradley et al. is composed of movement towards a fronto-parallel wall and a pursuit eye movement along the horizontal direction. The combination of these two movements and the geometry of the scene result in a flow that looks exactly like a pure expansion centered in the direction of gaze [see e.g. Fig. 1 c, f, i in (Lappe et al. 1999)]. This flow field is ambiguous (Regan and Beverly 1982; Longuet-Higgins 1984) and does not provide enough information to detect the presence of a rotational component. Human observers fail to identify the true heading in this condition (Warren and Hannon 1990; Grigo and Lappe 1999) and, in fact, respond very similarly to Bradley et al.'s neurons in that they erroneously report the shifted center or motion as their heading. This explains the lack of compensation for simulated pursuit that Bradley et al. found. However, when small instead of full field flow stimuli were used, visual cues to simulated rotation became available, such as the moving edges of the stimulus, and MST neurons partially compensated for the rotation (Shenoy et al. 1999).

In many neurons, the response modulation during real eye movements was smaller when compared with simulated eye movements. The neural basis of this difference in response modulation is as yet unclear, but may be due to changes in the attentional state of the animal between

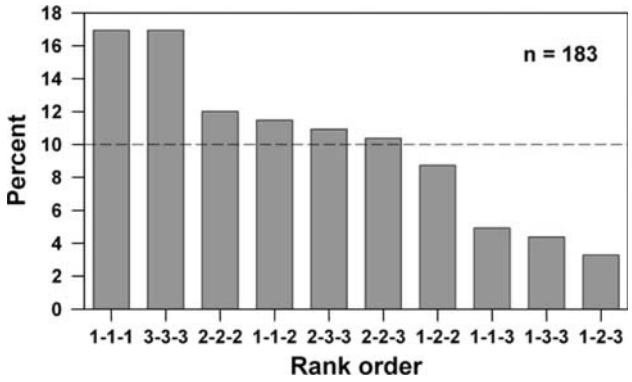

Fig. 5 Invariance of the heading responses for different eye movement conditions across the neuronal population. For each cell, we ranked for a given simulated eye movement (gain $g = 0.0$, 0.5, or 1.0) the responses of a neuron for each of the three simulated self-motion directions. This resulted in ten possible rank orders, i.e. a chance level of 10%. From each neuron with a significant tuning (number of neurons = 61), we obtained three rank orders (one for each self-motion direction). As an example, the responses for rightward motion as shown in Fig. 2 were strongest for $g = 0.0$ (rank = 1), $g = 0.5$ (rank = 1) and $g = 1.0$ (rank = 1), resulting in a rank order 1-1-1. Responses for straight-ahead motion were second largest in all three eye movement conditions (rank order 2-2-2). Responses for leftward motion were weakest in all three eye movement conditions (rank order 3-3-3). The responses of this neuron for the three self-motion directions hence resulted in the three rank orders 1-1-1, 2-2-2, and 3-3-3 and therefore were representative for the population of neurons ($n = 183$ rank orders). Invariances of heading responses were observed in 46% of the cases (1-1-1: 17%, 3-3-3: 17%, 2-2-2: 12%) and hence more often than expected by chance (30%). Switches of neuronal tuning indicated by rank orders 1-1-3, 1-3-3, or 1-2-3 were observed less frequently than predicted by chance (1-1-3: 4.9%, 1-3-3: 4.4%, 1-2-3: 3.3%, summing to a total of 12.6%). The neuronal discharges shown in Fig. 4 led to rank orders 1-1-2, 2-2-3, and 1-3-3

Table 2 Mean discharges and response ranks

	Leftward	Straight-ahead	Rightward
Gain 0.0	5.5/3	6.8/2	7.4/1
Gain 0.5	10.5/2	12.3/1	7.6/3
Gain 1.0	16.2/2	31.5/1	6.5/3
	2-2-3	1-1-2	1-3-3

Same convention as in Table 1; ranks were ordered by numerical values

conditions that required active fixation (simulated eye movement) and those that did not (real eye movement) (Treue and Maunsell 1996; Ben Hamed et al. 2002). It should be noted, however, that such an overall attentional shift should also influence the baseline activity, which was not observed in our study.

During real pursuit humans can use efference copy signals that allow the correct identification of heading. Likewise, the neurons in the study of Bradley et al. must have used an extraretinal eye movement signal to respond invariantly during real pursuit. Altogether, the condition used by Bradley et al. was ideally suited to demonstrate the use of an extraretinal signal for heading invariance in are MST, which is their major claim. However, these conditions would not allow studying a contribution of visual processes because the stimulus does not carry this information.

Our stimulus, in contrast to Bradley's, was specifically chosen because it has given the clearest evidence for the use of visual optic flow analysis in human studies. The combination of a ground plane with tracking eye movements has often been shown to allow good heading estimation (Warren and Hannon 1988, 1990; Van den Berg 1992, 1996), and is also particularly focused on in several modeling studies (Lappe and Rauschecker 1993; Perrone and Stone 1994; Lappe and Rauschecker 1995). We suspected it to be the best candidate for the initial demonstration of visual flow analysis in area MST. One should note, however, that several other factors (rotation speed: (Warren and Hannon 1990; Royden et al. 1992), depth order (Warren and Hannon 1990; Van den Berg 1996), field of view (Koenderink and Van Doorn 1987), and the presence of identifiable objects (Li and Warren 2000) are important for the estimation of heading from retinal flow, and that cues other than retinal flow can also be used for heading estimation (Llewellyn 1971; Cutting et al. 1997; Rushton et al. 1998).

The structure of the retinal flow pattern is an important factor for the estimation of self-motion and heading (Lappe et al. 1999). Because 3D scene layout and eye movements influence the structure of the retinal flow pattern, a single heading is associated with a large number of possible flow patterns. Among these patterns are simple radial expansions and spiraling motions. Both convey information about heading. Although MST neurons have been found to respond to both types of motion (Graziano et al. 1994; Duffy and Wurtz 1997) their relation has remained unclear. Our results suggest that the selectivities to expansion and spiral motion share a common goal and reflect the involvement of area MST in long range visual navigation.

Invariant heading responses require complicated visual tuning of heading detectors. The receptive field structure of MST neurons is not fully understood, but known to be complex (Duffy and Wurtz 1991b). The existence of neuronal mechanisms that determine heading visually from distorted flow fields has been proposed in several neural models for heading detection (Lappe and Rauschecker 1993; Perrone and Stone 1994; Beintema and Van den Berg 1998), but has not been tested before. Curiously, these models share the prediction of a bi-circular receptive field structure (Beintema et al. 2004). It will be interesting to see how the receptive fields of invariant heading detectors in MST are structured.

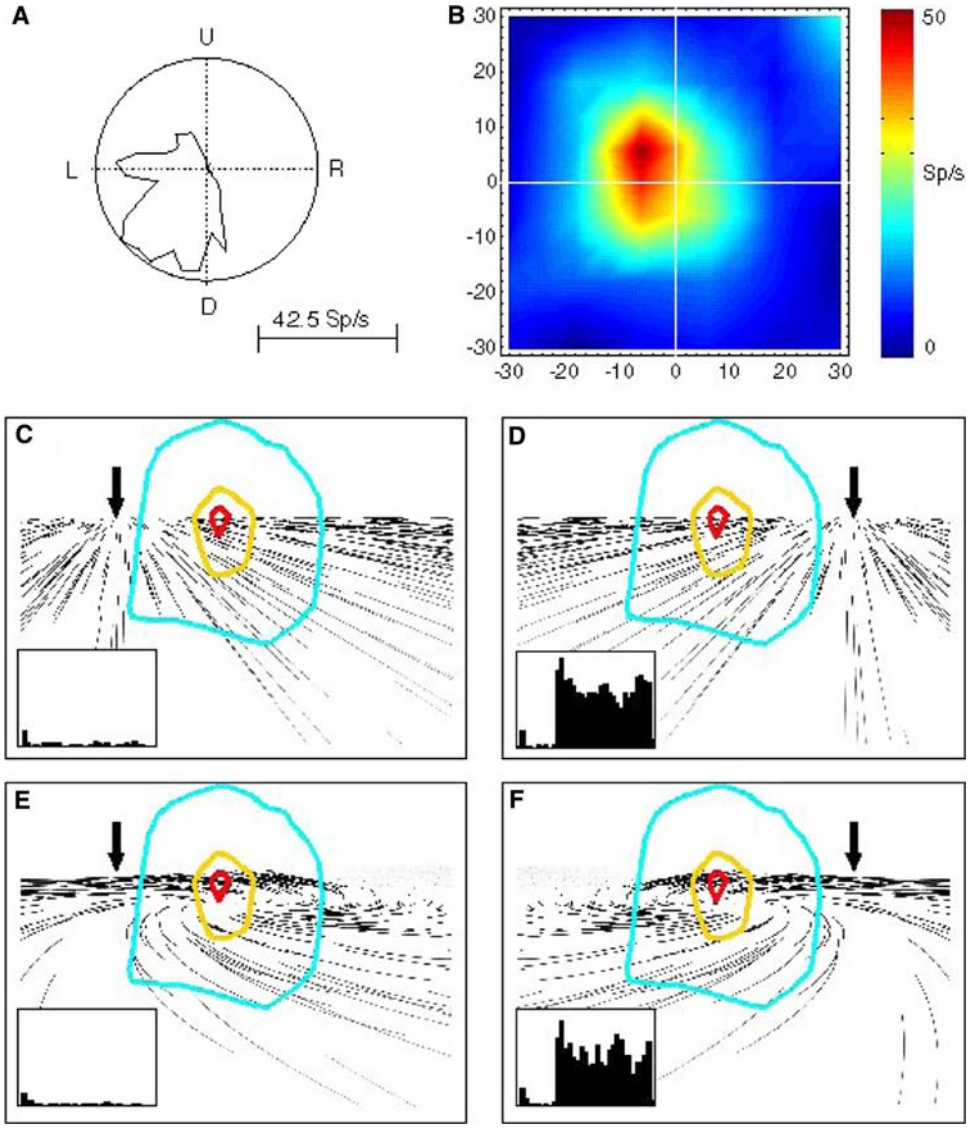

Fig. 6 Comparison between responses to unidirectional motion and optic flow in a single neuron. **a** Polar plot of directional selectivity for full field unidirectional motion. This neuron preferred left and downward motion. **b** Receptive field (RF) of the neuron when tested with luminant bars moving to the left. **c–f** Receptive field contours superimposed on flow stimuli for leftward (**c**, **e**) and rightward (**d**, **f**) heading and without (**c**, **d**) and with (**e**, **f**) simulated eye movements with gain 1. Respective responses to these stimuli are shown as *insets*. The neuron consistently responded to rightward heading and never to leftward heading, irrespective of simulated eye movements. In the lower part of the RF, image motion in both rightward heading stimuli is in the neuron's preferred direction. However, in the most sensitive part of the RF (RF center, outlined in *red*), which lies slightly left of the stimulus center at the horizon, the direction of local image motion changes. For pure radial flow with rightward heading (**d**), the local image motion at the RF center is to the left, consistent with the neuron's local image motion preference. With simulated eye movements (**f**), in contrast, local image motion in the RF center is to the right, yet the neuron fires with the same rate to optic flow. On the other hand, the neuron is silent for flow fields simulating leftward heading [without (**c**) or with (**e**) eye movements] even though local image motion in the RF center is to the left in the latter case (**e**)

Acknowledgments This work was supported by DFG-Sonderforschungsbereich 509.

References

Beintema JA, Van den Berg AV (1998) Heading detection using motion templates and eye velocity gain fields. Vision Res 38:2155–2179

Beintema JA, Van den Berg AV, Lappe M (2004) Circular receptive field structures for flow analysis and heading detection. In: Vaina LM, Beardsley SA, Rushton S (eds) The structure of receptive fields for flow analysis and heading detection. Kluwer Academic Publishers, Norwell, pp 223–248

Ben Hamed S, Duhamel JR, Bremmer F, Graf W (2002) Visual receptive field modulation in the lateral intraparietal area during attentive fixation and free gaze. Cereb Cortex 12:234–245

Bradley DC, Maxwell M, Andersen RA, Banks MS, Shenoy KV (1996) Mechanisms of heading perception in primate visual cortex. Science 273:1544–1547

Bremmer F, Ilg UJ, Thiele A, Distler C, Hoffmann KP (1997) Eye position effects in monkey cortex. I. Visual and pursuit-related

activity in extrastriate areas MT and MST. J Neurophysiol 77:944–961
Bremmer F, Kubischik M, Pekel M, Lappe M, Hoffmann KP (1999) Linear vestibular self-motion signals in monkey medial superior temporal area. Ann N Y Acad Sci 871(272–81):272–281
Bremmer F, Duhamel J-R, Ben Hamed S, Graf W (2002) Heading encoding in the macaque ventral intraparietal area (VIP). Eur J Neurosci 16:1554–1568
Britten KH, van Wezel RJ (1998) Electrical microstimulation of cortical area MST biases heading perception in monkeys. Nat Neurosci 1:59–63
Britten KH, van Wezel RJ (2002) Area MST and heading perception in macaque monkeys. Cereb Cortex 12:692–701
Cutting JE, Vishton PM, Fluckiger M, Baumberger B, Gerndt JD (1997) Heading and path information from retinal flow in naturalistic environments. Percept Psychophys 59:426–441
Duffy CJ, Wurtz RH (1991a) Sensitivity of MST neurons to optic flow stimuli. I. A continuum of response selectivity to large-field stimuli. J Neurophysiol 65:1329–1345
Duffy CJ, Wurtz RH (1991b) Sensitivity of MST neurons to optic flow stimuli. II. Mechanisms of response selectivity revealed by small-field stimuli. J Neurophysiol 65:1346–1359
Duffy CJ, Wurtz RH (1997) Planar directional contributions to optic flow responses in MST neurons. J Neurophysiol 77:782–796
Duhamel JR, Bremmer F, BenHamed S, Graf W (1997) Spatial invariance of visual receptive fields in parietal cortex neurons. Nature 389:845–848
Erickson RG, Thier P (1991) A neuronal correlate of spatial stability during periods of self-induced visual motion. Exp Brain Res 86:608–616
Froehler MT, Duffy CJ (2002) Cortical neurons encoding path and place: where you go is where you are. Science 295:2462–2465
Galletti C, Squatrito S, Battaglini PP, Grazia MM (1984) 'Real-motion' cells in the primary visual cortex of macaque monkeys. Brain Res 301:95–110
Galletti C, Battaglini PP, Aicardi G (1988) 'Real-motion' cells in visual area V2 of behaving macaque monkeys. Exp Brain Res 69:279–288
Galletti C, Battaglini PP, Fattori P (1990) 'Real-motion' cells in area V3A of macaque visual cortex. Exp Brain Res 82:67–76
Gibson JJ (1950) The perception of the visual world. Houghton Mifflin, Boston
Graziano MS, Andersen RA, Snowden RJ (1994) Tuning of MST neurons to spiral motions. J Neurosci 14:54–67
Grigo A, Lappe M (1999) Dynamical use of different sources of information in heading judgments from retinal flow. J Opt Soc Am A Opt Image Sci Vis 16:2079–2091
Gu Y, Watkins PV, Angelaki DE, DeAngelis GC (2006) Visual and nonvisual contributions to three-dimensional heading selectivity in the medial superior temporal area. J Neurosci 26:73–85
Gu Y, Angelaki DE, DeAngelis GC (2008) Neural correlates of multisensory cue integration in macaque MSTd. Nat Neurosci 11:1201–1210
Judge SJ, Richmond BJ, Chu FC (1980) Implantation of magnetic search coils for measurement of eye position: an improved method. Vision Res 20:535–538
Koenderink JJ, Van Doorn AJ (1987) Facts on optic flow. Biol Cybern 56:247–254
Lagae L, Maes H, Raiguel S, Xiao DK, Orban GA (1994) Responses of macaque STS neurons to optic flow components: a comparison of areas MT and MST. J Neurophysiol 71:1597–1626
Lappe M, Rauschecker JP (1993) A neural network for the processing of optic flow from ego-motion in man and higher mammals. Neural Comput 5:374–391 Ref Type: Generic
Lappe M, Rauschecker JP (1994) Heading detection from optic flow. Nature 369:712–713
Lappe M, Rauschecker JP (1995) Motion anisotropies and heading detection. Biol Cybern 72:261–277
Lappe M, Bremmer F, Pekel M, Thiele A, Hoffmann KP (1996) Optic flow processing in monkey STS: a theoretical and experimental approach. J Neurosci 16:6265–6285
Lappe M, Pekel M, Hoffmann K-P (1998) Optokinetic eye movements elicited by radial optic flow in the macaque monkey. J Neurophysiol 79:1461–1480
Lappe M, Bremmer F, Van den Berg AV (1999) Perception of self motion from visual flow. Trends Cogn Sci 3:329–336
Li L, Warren WH Jr (2000) Perception of heading during rotation: sufficiency of dense motion parallax and reference objects. Vision Res 40:3873–3894
Llewellyn KR (1971) Visual guidance of locomotion. J Exp Psychol 91:245–261
Longuet-Higgins HC (1984) The visual ambiguity of a moving plane. Proc R Soc Lond B Biol Sci 223:165–175
Morgan ML, DeAngelis GC, Angelaki DE (2008) Multisensory integration in macaque visual cortex depends on cue reliability. Neuron 59:662–673
Page WK, Duffy CJ (1999) MST neuronal responses to heading direction during pursuit eye movements. J Neurophysiol 81:596–610
Perrone JA, Stone LS (1994) A model of self-motion estimation within primate extrastriate visual cortex. Vision Res 34:2917–2938
Regan D, Beverly KI (1982) How do we avoid confounding the direction we are looking and the direction we are moving? Science 215:194–196
Royden CS, Banks MS, Crowell JA (1992) The perception of heading during eye movements. Nature 360:583–585
Rushton SK, Harris JM, Lloyd MR, Wann JP (1998) Guidance of locomotion on foot uses perceived target location rather than optic flow. Curr Biol 8:1191–1194
Schlack A, Sterbing-D'Angelo SJ, Hartung K, Hoffmann KP, Bremmer F (2005) Multisensory space representations in the macaque ventral intraparietal area. J Neurosci 25:4616–4625
Schoppmann A, Hoffmann K-P (1976) Continuous mapping of direction selectivity in the cat's visual cortex. Neurosci Lett 2:177–181
Shenoy KV, Bradley DC, Andersen RA (1999) Influence of gaze rotation on the visual response of primate MSTd neurons. J Neurophysiol 81:2764–2786
Tanaka K, Saito H (1989) Analysis of motion of the visual field by direction, expansion/contraction, and rotation cells clustered in the dorsal part of the medial superior temporal area of the macaque monkey. J Neurophysiol 62:626–641
Treue S, Maunsell JH (1996) Attentional modulation of visual motion processing in cortical areas MT and MST. Nature 382:539–541
Upadhyay UD, Page WK, Duffy CJ (2000) MST responses to pursuit across optic flow with motion parallax. J Neurophysiol 84:818–826
Van den Berg AV (1992) Robustness of perception of heading from optic flow. Vision Res 32:1285–1296
Van den Berg AV (1993) Perception of heading. Nature 365:497–498
Van den Berg AV (1996) Judgements of heading. Vision Res 36:2337–2350
Warren WH, Hannon DJ (1988) Direction of self-motion is perceived from optical flow. Nature 336:162–163
Warren WHJ, Hannon DJ (1990) Eye movements and optical flow. J Opt Soc Am [A] 7:160–169
Wei M, Angelaki DE (2006) Foveal visual strategy during self-motion is independent of spatial attention. J Neurosci 26:564–572